The *Ralstonia solanacearum* pathogenicity regulator HrpB induces 3-hydroxy-oxindole synthesis

Fabien Delaspre*, Carlos G. Nieto Peñalver*†, Olivier Saurel‡, Patrick Kiefer†, Emmanuel Gras§, Alain Milon‡, Christian Boucher*, Stéphane Genin*, and Julia A. Vorholt*†¶

*Laboratoire des Interactions Plantes Micro-Organismes (LIPM), Institut National de la Recherche Agronomique/Centre National de la Recherche Scientifique, BP52627, 31326 Castanet-Tolosan, France; †Institute of Microbiology, Eidgenössische Technische Hochschule Zurich, 8093 Zurich, Switzerland; ‡Institute of Pharmacology and Structural Biology, University of Toulouse, UPS-Centre National de la Recherche Scientifique, 31077 Toulouse, France; and §University of Toulouse, UPS–Centre National de la Recherche Scientifique, Laboratoire de Synthèse et PhysicoChimie des Molécules d'Intérêt Biologique, Université Paul Sabatier, 31062 Toulouse, France

Edited by Frederick M. Ausubel, Harvard Medical School, Boston, MA, and approved August 14, 2007 (received for review January 30, 2007)

The transcriptional activator HrpB of the bacterial wilt causing betaproteobacterium *Ralstonia solanacearum* represents a key regulator for pathogenicity. In particular, it drives expression of *hrp* genes encoding a type III secretion system (T3SS) as well as effector molecules for delivery into the host cytosol to promote disease. However, the HrpB regulon extends beyond this T3SS. We describe here an HrpB-activated operon of six genes that is responsible for the synthesis of a fluorescent isatin derivative of 149 Amu that we named HDF for HrpB-dependent factor and that we purified from culture supernatants. The structure of the labile molecule was solved by using NMR and CD spectroscopy to be (3*S*)-3-hydroxy-indolin-2-one and confirmed by its chemical synthesis and MS spectrometry. HDF was found to be present at 20 nM in wild-type cultures grown on minimal medium, and its synthesis increased 15-fold upon overproduction of HrpB, confirming that HrpB activates HDF synthesis. The addition of tryptophan significantly stimulated HDF biosynthesis and was shown to represent the precursor molecule for HDF synthesis. A search for the biological function of the molecule revealed that HDF induces acyl-homoserine lactone receptor-mediated reporter activity of the well studied LuxR transcriptional regulator of *Vibrio fischeri*. Thus, our results provide evidence that the specificity of acyl-homoserine lactone (acyl-HSL) receptors is clearly broader than previously considered. The failure to detect induction by HDF of the described endogenous quorum-sensing circuits of the pathogen points to a role in interfering with cell–cell signaling of rivalling bacteria.

plant pathogen | tryptophan | isatin | quorum sensing | cell–cell communication

Ralstonia solanacearum is a devastating plant pathogen with wide geographic distribution and an unusually wide host range because it is the agent of vascular wilt disease in >200 plant species (1). After entering plant roots, the pathogen invades the xylem vessels and rapidly spreads to aerial parts of the plant throughout the vascular system. Typical wilting symptoms result from an excessive production of extracellular polysaccharides within the vascular system, altering water fluxes in the plant. Molecular and genetic approaches have identified a wide range of genes and functions required for the development of the disease (2, 3). Among them, a key determinant of *R. solanacearum* pathogenicity is the type III secretion system (T3SS) that allows the translocation of effector proteins into plant cells (2). T3SS-defective mutants are unable to cause disease symptoms on host plants.

The expression of *R. solanacearum* T3SS-encoding and effector genes is activated in response to bacterium-plant cell contact through a six-gene regulatory cascade (4, 5). At the bottom of this cascade is HrpB, an AraC family regulator, which activates T3SS-encoding and effector genes via the hrp_{II} box cis-element (6). Recently, transcriptome analysis of a *hrpB* mutant revealed that the HrpB regulator not only controls the expression of T3SS biosynthesis genes, and probably >60 effector substrates, but also functions that extend beyond the T3SS-dependent export pathway (7). The coordinated expression of these genes with the T3SS and effector genes through HrpB suggests that they might encode functions important for pathogenicity and/or during the infection of plants.

In the present study, we performed a functional analysis of an HrpB-activated operon comprising six genes predicted to encode small molecule metabolism enzymes. This six-gene operon is located 200 kb away from the *hrp* gene cluster of strain GMI1000 (8) and contains within its promoter the HrpB-dependent hrp_{II} box control element (located 450 bp upstream of the start codon of the RSp0693 gene). These genes do not seem to encode substrates of the T3SS because none of the corresponding proteins harbor predicted T3SS-export signals (9). Here, we demonstrate that these genes are responsible for the synthesis of a tryptophan derivative, HDF (HrpB-dependent factor), which accumulates in the spent medium. We show that HDF exhibits cross-reactivity with a heterologous LuxR receptor for small molecule signals of the acyl-homoserine lactone (acyl-HSL) family of Gram-negative bacteria (10). These autoinducer molecules are involved in the regulation of bacterial physiology in a cell-density dependent manner in a process known as quorum sensing. The HDF-mediated acyl-HSL receptor activity of HDF creates a link between HrpB-driven pathogenicity to signaling and cell–cell communication and extends the specificity of LuxR transcription factors to a previously undescribed family of ligands.

Results

Detection of a Fluorescent Molecule Produced by Enzymes Encoded in the HrpB-Dependent *hdf* Operon. The RSp0693-RSp0698 genes of *R. solanacearum* are organized in a conspicuous HrpB-regulated operon (7). The predicted gene products fall into the class of small molecule metabolism and are predicted to encode glyoxylase I (RSp0693), tryptophan-2,3 dioxygenase (RSp0694), a dehydrogenase (RSp0695), an epimerase (RSp0696), a short chain dehydrogenase (RSp0697), and an aminotransferase (RSp0698), respectively. These gene functions led us to hypothesize that they might

Author contributions: F.D. and C.G.N.P. contributed equally to this work; F.D., C.G.N.P., O.S., A.M., C.B., S.G., and J.A.V. designed research; F.D., C.G.N.P., O.S., P.K., E.G., S.G., and J.A.V. performed research; O.S., P.K., and E.G. contributed new reagents/analytic tools; F.D., C.G.N.P., O.S., P.K., A.M., C.B., S.G., and J.A.V. analyzed data; and F.D., C.G.N.P., O.S., S.G., and J.A.V. wrote the paper.

The authors declare no conflict of interest.

This article is a PNAS Direct Submission.

Abbreviations: T3SS, type III secretion system; HDF, HrpB-dependent factor; HSL, homoserine lactone; HSQC, heteronuclear single quantum correlation; LC-MS, liquid chromatography mass spectrometry; Rf, retention factor.

¶To whom correspondence should be sent: ETH Zurich, Institute of Microbiology, Hoenggerberg HCI, Wolfgang-Pauli-Strasse 10, 8093 Zurich, Switzerland. E-mail: vorholt@micro.biol.ethz.ch.

This article contains supporting information online at www.pnas.org/cgi/content/full/0700782104/DC1.

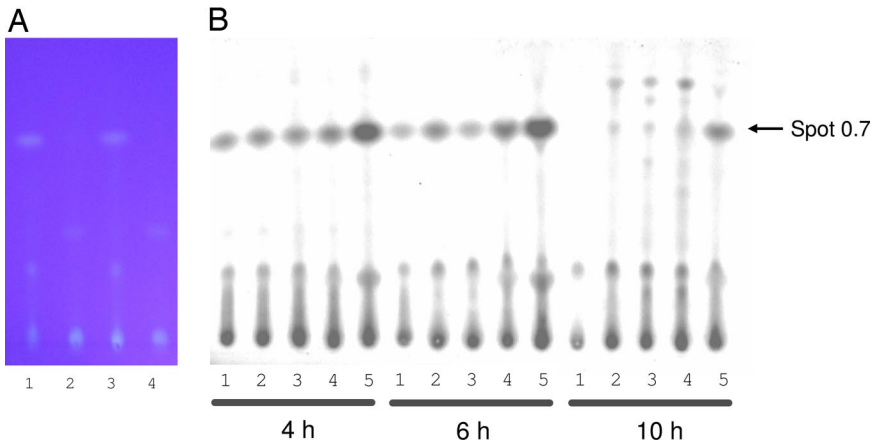

Fig. 1. Analysis of extracts from *R. solanacearum* culture supernatants. (*A*) Photograph of a TLC chromatogram upon revelation by UV light after separation of extracts from culture supernatants of *R. solanacearum* grown on minimal medium: (lane 1) GMI1000 wild-type cells (1 μl of 1,000 times concentrated extract); (lane 2) *hrpB* deficient GMI1525 (1 μl of 1000 times concentrated extract); (lane 3) *hrpB*-overexpressing GMI1728 (1 μl of 200 times concentrated extract); (lane 4) RSp0694 deficient GRS407 (1 μl of 1000 times concentrated extract). Comparison of thin-layer chromatograms of concentrated supernatant extracts from these strains revealed that the GMI1000 and GMI1728 extracts contain a yellow-fluorescing spot under UV light that migrated at an Rf value of 0.7. (*B*) TLC chromatogram upon revelation by UV light after separation of extracts from culture supernatants of *R. solanacearum* GMI1728 grown on minimal medium after addition of various amounts of tryptophan (lane 1, 0 mM; lane 2, 0.25 mM; lane 3, 0.5 mM; lane 4, 1 mM; lane 5, 5 mM) and three different induction times (4 h, 6 h, and 10 h).

represent the biosynthetic pathway of a tryptophan derivative with tryptophan-2,3 dioxygenase (11) catalyzing the initial step. Furthermore, we speculated that the molecule might accumulate in the culture supernatant and eventually be recognizable as a colored or fluorescent compound.

To test these assumptions we grew *R. solanacearum* GMI1000 wild-type cells and several GMI1000 derivatives in minimal medium, a condition that is known to induce *hrpB* expression (12), and extracted and analyzed culture supernatants. Among the GMI1000 derivatives tested were GMI1728, which contains pAM5 for *hrpB* overexpression (13), and the strain GMI1525, a *hrpB*-deficient mutant derivative (12). In addition, we constructed a GRS407 strain that contains a disruption in its RSp0694 gene by an omega interposon resulting in abolished transcription of RSp0694 to RSp0698 (results not shown). Comparison of thin-layer chromatograms of concentrated culture supernatant extracts from these strains revealed that GMI1000 extracts contain a yellow-fluorescing spot under UV light that migrates at a retention factor (Rf) value of 0.7 under our separation conditions (Fig. 1*A*). The intensity of the spot was greater in the GMI1728 strain but was undetectable in the chromatograms of the GMI1525 and GRS407 strains (Fig. 1*A*). To ensure that the mutation in GRS407 abolished the production of the yellow-fluorescing spot completely, we introduced pAM5 in the GRS407 background. In extracts of this *hrpB*-overexpressing but RSp0694 mutant strain, the Rf = 0.7 spot was also not detectable. Semipreparative HPLC analysis followed by TLC chromatography and UV detection confirmed the correlation of the production of the yellow-fluorescing substance as dependent on the intact RSp0694-RSp0698 operon as well as *hrpB* expression. Thus, we named the compound HDF for HrpB-dependent factor.

The detection of HDF in the supernatant of strain GMI1694, a *hrcV* T3SS-secretion mutant (9), was similar to that observed in the supernatant of the wild-type strain, indicating that the secretion of this molecule is not mediated by the T3SS. Extraction of whole cultures instead of spent medium resulted in slightly increased intensities of the HDF fluorescing spot. However, we continued to work with culture supernatants for the rest of the study because of lower complexity of the extracts (data not shown).

The identification of RSp0693-0698 as the genes responsible for HDF (i.e., *hdf* genes) was further substantiated by expression studies in *Escherichia coli*. The yellow-fluorescing spot could also be observed upon TLC of HPLC-fractionated culture supernatants of the *E. coli* strain harboring the RSp0693-0698 genes under the control of the *lac* promoter and not the control strain harboring empty vector. This experiment shows that the *hdf* cluster is responsible and sufficient for the production of HDF. The apparent amount of HDF detected in extracts of *E. coli* culture supernatants was not significantly higher than that of *R. solanacearum* cultures and further work concentrated on extracts obtained from *R. solanacearum*.

Purification of HDF Reveals Its Nature as a Labile Compound. We aimed to optimize the amount of HDF produced to facilitate its purification for structural analysis and biological tests. Therefore we tested with the GMI1728 strain whether supplementation of tryptophan leads to increased production of HDF. Overnight cultures were divided and a range of different concentrations of tryptophan were added. Culture samples were taken at 4, 6, and 10 h and analyzed (Fig. 1*B*). We observed that an increase of tryptophan concentration up to 5 mM leads to an increase in HDF production. However, higher concentrations of tryptophan resulted in a negative effect on bacterial growth and concomitant decrease in HDF production (data not shown). We observed a slight increase in production after 6 h of tryptophan supplementation. During prolonged growth of >6 h, HDF concentration apparently decreased (Fig. 1*B*).

For standard purification of HDF, we incubated overnight cultures of the GMI1728 strain, added 5 mM tryptophan and collected culture supernatants after an additional 6 h. Purification of HDF was optimized and established within two chromatographic steps as described in Experimental Procedures. The fluorescing intensity of purified HDF diminished rapidly at 4°C and resulted in a yellow nonfluorescing compound, indicating that HDF is unstable. Therefore, extraction of HDF was accomplished from fresh supernatants without previous freezing, and both chromatographic steps were performed the following day. Purified samples were then stored in acetonitrile at −80°C until further analysis.

Identification of HDF as (3*S*)-3-Hydroxy-Indolin-2-One by NMR and CD Spectroscopy. Initial one and two dimensional ^{1}H-^{1}H COSY NMR spectra of purified HDF in D_2O revealed only four peaks characteristic of an 1,2-di-substituted aromatic ring. But the lack of proton

MICROBIOLOGY

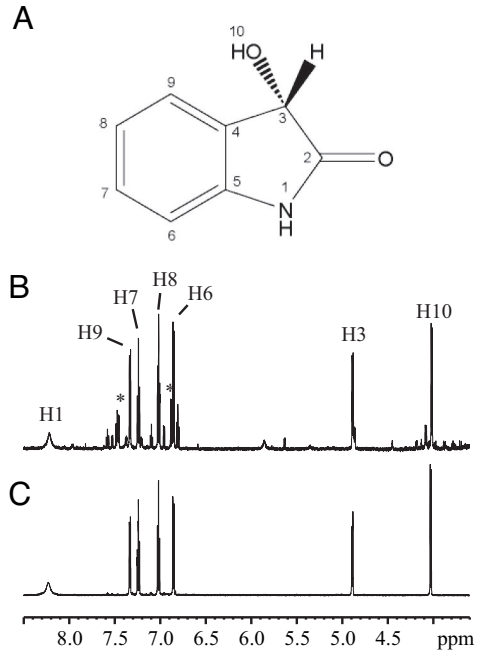

Fig. 2. Proton NMR spectra of purified and synthesized 3-hydroxy-oxindole. (*A*) Chemical structure of HDF. (*B*) ^{1}H NMR spectrum of HDF extracted and purified from the growth medium. (*C*) ^{1}H NMR spectrum of chemically synthesized 3-hydroxy-1,3-dihydro-2*H*-indol-2-one. Spectra were performed at 18°C in acetonitrile-d_3. The displayed region 8.5–3.5 ppm is limited to observable HDF signals. ^{1}H resonances are labeled according to the numbering illustrated in *A*.

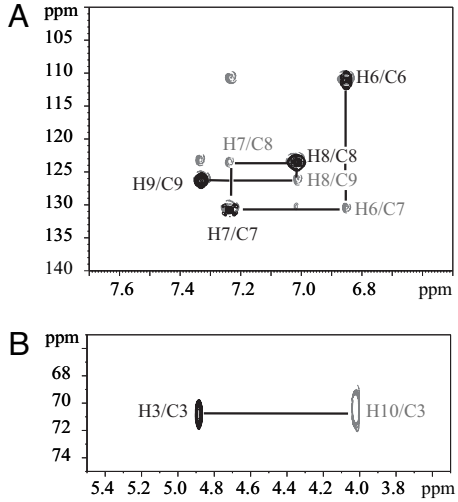

Fig. 3. Proton and carbon resonance assignment of HDF using heteronuclear correlation NMR spectroscopy. (*A*) Expanded region ($\delta F2$ 7.7–6.5 ppm and $\delta F1$ 140–100 ppm) and (*B*) ($\delta F2$ 5.5–3.5 ppm and $\delta F1$ 75–65 ppm) of the ^{1}H-^{13}C HSQC and H2BC spectra of U-[^{15}N,^{13}C] HDF at 18°C in acetonitrile-d_3. HSQC (black contour lines) and H2BC (gray contour lines) are superimposed. H2BC is based on two-bond ^{1}H-^{13}C correlations allowing for sequential assignment using both ^{1}H and ^{13}C resonances. To illustrate sequential assignment, important correlation peaks are connected with lines and labeled according to the ^{1}H and ^{13}C resonances associated with the atom numbering.

resonances other than the aromatic ones suggested the presence of a short substituted moiety, probably composed of functional groups with exchangeable protons.

Further NMR analyses for structural assessment were hindered by the limited amount of purified product in combination with compound instability: indeed, we observed a continuous shift of the four proton aromatic signals over one week in our experimental conditions. We improved sample stability by solubilizing HDF in acetonitrile and carefully de-gassing the solution to prevent putative hydrolysis and/or oxidation. At the same time, the aprotic solvent acetonitrile enabled us to observe the resonances of exchangeable protons. To obtain information on hetero-atoms using experiments with low sensitivity such as HMBC, we prepared uniformly labeled ^{13}C and ^{15}N HDF (U-[^{15}N,^{13}C] HDF). To this end, we purified HDF from GMI1728 cultures containing U-[^{15}N,^{13}C] glutamate as a unique carbon source and supplemented the growth medium with U-[^{15}N,^{13}C] tryptophan.

A complete set of one and two dimensional NMR experiments was performed with U-[^{15}N,^{13}C] HDF in acetonitrile resulting in the identification of 3-hydroxy-1,3-dihydro-2*H*-indol-2-one as HDF (Fig. 2*A*). The 1D ^{1}H and 2D ^{1}H-^{1}H COSY spectra revealed two distinct spin systems, one was the aromatic region as previously observed and the second was in the region from 5 to 4 ppm (Fig. 2*B*). These spin systems were completely characterized by using both the proton and the carbon chemical shifts using 2D ^{1}H-^{13}C heteronuclear single quantum correlation (HSQC)/H2BC experiments (14). Assignment of carbon resonances bound to protons resulted directly from the analysis of the HSQC spectrum, whereas the H2BC correlated protons and carbon spins separated by two covalent bonds. As shown in Fig. 3*A*, peak H6/C6 (HSQC) correlated with H6/C7 (H2BC), H7/C7 correlated with H7/C8 and H8/C8 correlated with H8/C9. In the region from 5 to 4 ppm (δ_{1H}) only peak H3/C3 appeared in the HSQC, and no peak was observed at 4.02 ppm (H10), demonstrating H10 is not bound to a carbon.

Moreover, ^{1}H-^{1}H COSY and H2BC spectra revealed a cross peak between H10/H3 and H10/C3, respectively (Fig. 3*B*). Based on coupling observations and chemical shift values, the resonances could be assigned to the proton of a methine group (4.88 ppm, H3) bound to a hydroxyl group (4.01 ppm, H10). These signals were not observed in D_2O solvent because the hydroxyl proton vanished in the spectrum because of chemical exchange with D_2O and resonance at 4.88 ppm overlapped with the intense signal of residual HDO. Besides the two spin systems, an additional proton signal at 8.22 ppm appeared in acetonitrile, corresponding to an amide proton, because it was a doublet with a coupling constant of 90 Hz characteristic of a $^{1}J_{1H\text{-}15N}$ scalar coupling constant.

Complete assignment of the carbon skeleton, including quaternary carbon atoms and their connectivities, was performed by using 1D carbon detected, ^{1}H-^{13}C HMBC experiments. The carbonyl carbon (C2) was identified because of its correlation with protons H10 and H3 [supporting information (SI) Fig. 5]. Furthermore, the position of the α-hydroxy-ketone moiety was characterized by correlation of H10 and H3 with C4. Position of the substitutes was confirmed both by analysis of the one bond ^{13}C-^{13}C scalar coupling constants in the 1D carbon detected spectrum (SI Fig. 6) and by sequential correlations C3-C4-C9-C8-C7-C6-C5 in the ^{13}C-^{13}C COSY spectrum.

At this level of the analysis, all proton and carbon resonances could be unambiguously assigned (SI Table 1). However, it remained unclear whether the carbonyl carbon belonged to a carboxylic acid or was involved in an amide group resulting in an indole structure. To address this issue, we performed 2D versions (^{1}H-^{15}N and ^{1}H-^{13}C) of an 3D HN(CO)CA experiment. Only if ^{15}N,^{13}C-HDF is an indole ring, the magnetization has to be transferable from the amide proton to the C3 carbon via the C2 carbonyl. The experiments showed one correlation peak at δ_{1H} = 8.22 ppm with δ_{15N} = 116.9 ppm and with δ_{13C} = 70.7 ppm (SI Fig. 7), demonstrating that HDF was the 3-hydroxy-indolin-2-one illustrated in Fig. 2*A*.

NMR analysis revealed the chemical structure of HDF, except for the absolute configuration of the 3-hydroxyl group. The chirality of the (3*R*)-3-hydroxy-5-methyl-indolin-2-one was determined by

using circular dichroism (CD) spectroscopy and quantum chemical calculation (15). The CD spectrum of HDF in ethanol was recorded and revealed the same spectrum but with opposite sign, in agreement with an *S* absolute configuration (data not shown). Therefore, the chemical structure of the natural extract of HDF from *R. solanacearum* was (3*S*)-3-hydroxy-1,3-dihydro-2*H*-indol-2-one.

Confirmation of HDF Structure by Liquid Chromatography Mass Spectrometry and Chemical Synthesis. HDF purified from *R. solanacearum* was also analyzed by liquid chromatography mass spectrometry (LC-MS). An ion with an *m/z* value of 150.0548 was detected eluting after 3.09 min (SI Fig. 8*A*). The formula of the ion was determined as $C_8O_2N_1H_8$ with a mass deviation below 1 ppm which corresponds to the $[M+H]^+$ ion of HDF.

To unambiguously confirm the chemical structure of HDF, we synthesized racemic 3-hydroxy-indolin-2-one by means of reduction of isatin by sodium borohydride (16). Synthetic product was analyzed by ^1H and ^{13}C NMR as well as LC-MS and gave a spectrum, *m/z* value and retention time, respectively, identical to the natural purified HDF (Fig. 2*C*; SI Fig. 8*B*).

Confirmation of Tryptophan as a Precursor Molecule for HDF Production. As indicated above, the addition of tryptophan to the *R. solanacearum* cultures resulted in higher amounts of the yellow-fluorescing spot of HDF. By means of LC-MS we confirmed that the addition of 5 mM tryptophan resulted in a 5-fold increased amount of HDF in supernatants of wild-type cultures from 20 nM to 100 nM and a 2.5-fold increased concentration from 300 to 750 nM of the *hrpB* overexpressing strain GMI1728.

To directly show that tryptophan is the precursor for HDF synthesis, we purified and characterized HDF from GMI1728 to which 5 mM of U-[^{15}N,^{13}C]-tryptophan was added. A mass peak of $[M+H]^+$ at *m/z* 159 was found in agreement with a mass shift of +9 relative to [^{14}N,^{12}C]-HDF (data not shown). However, extractions from tryptophan labeled cultures also contained a minor mass peak of *m/z* 150 indicating that HDF is partially also synthesized from endogenous unlabeled tryptophan.

HDF Induces Reporter Activity of an Exogenous LuxR Protein but Does Not Affect the Endogenous Quorum-Sensing Circuits. HrpB is known as a master regulator that governs physiological status of saprophytic to parasitic lifestyle in *R. solanacearum* (7). HrpB-dependent expression of *hdf* genes and the concomitant synthesis of HDF raised the question of whether this small tryptophan-derived molecule acts as a signal to the host plant or among the *R. solanacearum* population at this critical point of infection or whether it acts on other concurrent bacteria that might benefit from the attack of this pathogen. We observed that the infiltration of HDF into plant leaves (*Arabidopsis*, tobacco, and tomato) did not elicit any phenotypic response and found no evidence that HDF exhibits antibiotic activity in preliminary tests, nor could we observe any effect on growth of *R. solanacearum*. We investigated the possibility that HDF might be involved in bacterial cell–cell communication and tested whether HDF cross-reacts with a classical quorum-sensing system that is based on a acyl-HSL receptor, similar to certain cyclic dipeptides that can induce the activity of several LuxR homologs (17, 18). We performed tests with an *E. coli* strain containing the pSB401 plasmid (19) which is based on bioluminescent reporter activity. We were able to demonstrate that the LuxR receptor of *Vibrio fischeri* is induced in the presence of HDF (Fig. 4). Thus, HDF clearly represents a previously undescribed group of molecule that is very structurally dissimilar to the family of acyl-HSL and is capable of inducing LuxR receptor activity.

Quantitative assays with the *E. coli* pSB401 strain were performed as described (19) and showed that reporter gene activity was linear upon addition of 0.3–1.4 nmol HDF. Also synthetic HDF showed linear dose dependence in the same concentration range; however the light intensity was generally lower probably because of the presence of the two stereoisomers in the chemical product but only one, the *S*-stereo conformation in the naturally occurring HDF. Further evidence that HDF acts highly specific was obtained from assays in which we tested isatin that is structurally closely related to HDF and its degradation product as revealed by NMR experiments. No reporter activity in *E. coli* pSB401 upon addition of isatin could be revealed.

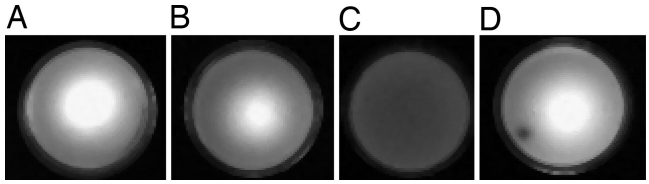

Fig. 4. Bioassay of purified HDF from *R. solanacearum* spotted on Petri dishes using *E. coli* pSB401 as an indicator strain. Samples were spotted onto the center of the plates as follows: HDF (7.5×10^{-10} mol) (*A*); HDF (2×10^{-10} mol) (*B*); acetonitrile (*C*); and *N*-hexanoyl-homoserine lactone standard (10^{-10} mol) (*D*).

To investigate the degree of specificity of LuxR proteins for induction by HDF, we tested other described bioreporter assays (see *Experimental Procedures*). None of the strains tested showed LuxR-dependent activation by HDF. Consistently with the result of induction of reporter gene activity of LuxR from *V. fischeri* in *E. coli* pSB401, a positive response was found when using the pSB403 reporter (19) or when using GFP as a reporter gene of the same LuxR receptor in *E. coli* MT102 (pJBA-132) (20) (data not shown). We then analyzed whether HDF could exert an inhibitory activity against acyl-HSL autoinducer molecules in various biosensor strains. Except one, HDF showed no antagonistic effect in any of the conditions analyzed. Only for *Agrobacterium tumefaciens* NTL4 (pCF218)(pCF372) containing a LuxR homolog that is inducible by *N*-hexanoyl-HSL (21), a 20% and a 40% reduced reporter activity relative to the control assay was observed when HDF was added in 5- and 10-fold excess, respectively.

The *R. solanacearum* genome exhibits the presence of two couples of *luxI*/*R* homologs (RSc3286, RSc3287, RSp0778, and RSp0779) which are involved in the biosynthesis of *N*-hexanoyl-HSL and *N*-octanoyl-HSL (22). Besides these classical acyl-HSL molecules, *R. solanacearum* was shown to produce 3-hydroxypalmitic acid methyl ester (3-OH PAME) as a molecule involved in cell–cell signaling (23). To investigate whether HDF acts on its endogenous quorum-sensing systems, we quantified acyl-HSL and 3-OH PAME, respectively, under various conditions. However, no difference in concentration of these autoinducer molecules was observed when extracts from GMI1000 wild-type cells were compared with extracts from GRS407 as well as the GMI1000 pAM5 (GMI1728) to GRS407 pAM5. Also the addition of HDF to cultures of wild-type cells did not alter quantities of acyl-HSL and 3-OH PAME in extracts from culture supernatants. Thus, HDF does not seem to act on its endogenous quorum-sensing circuits, but on exogenous LuxR receptor in a rather specific manner.

Discussion

HrpB of *R. solanacearum* represents a key regulator of pathogenicity-related gene functions. It strongly activates transcription of RSp0693-0698 genes (7), including Rsp0694 expression as assessed by using a genetic screen (24). The present study shows that the RSp0693-0698 genes, now termed *hdf* genes, are responsible for the synthesis of a small molecular mass compound of 149 Amu that we identified as (3*S*)-3-hydroxy-indolin-2-one. The finding that the synthesis of HDF depends on the T3SS regulator HrpB but that its secretion into the medium is T3SS-independent confirms that HrpB governs the expression of genes that extend beyond T3S machinery and effectors. It is very likely that *hdf* expression is mediated directly by HrpB because the conserved hrp_{II} box control element is located upstream of the first *hdf* gene in the operon. The

observation that *hdf* genes are conserved in 17 *R. solanacearum* strains representative of the genetic diversity of the species (25) indicates that these genes belong to the "core genome," which supports the hypothesis that these genes may be important for the fitness of the pathogen.

Further homology searches revealed that the *hdf* operon is highly conserved in another plant pathogenic strain of *Xanthomonas campestris* pv. *campestris* (26). Gene organization is similar in the two organisms and the homology at the nucleotide level is >80% over most of the operon, suggesting the occurrence of a lateral gene transfer event. Interestingly, the *hdf* operon in *X. campestris* pv. *campestris* is part of the *hrp* pathogenicity island that also contains the T3SS genes. This physical linkage, in addition to the coregulation of *hdf* and T3SS genes observed in *R. solanacearum*, suggests a role of the *hdf* genes during plant colonization although the *hdf* disruption mutant remained pathogenic under our experimental test conditions (data not shown). It is therefore probable that HDF may play a more subtle role at certain point(s) of the pathogenic lifestyle *of R. solanacearum*.

An indication that HDF is involved in bacterial cell–cell signaling stems from our finding that HDF induces the activity of a classical LuxR receptor. So far, the only identified natural non acyl-HSL molecules that can stimulate LuxR receptors are certain cyclic dipeptides (17, 18). However, it should be noted that, within a large-scale screen of synthetic molecules, triphenyl compounds were identified that also act as activators of a LuxR homologue (27). Our results broaden the group of structurally characterized bacterial small molecules involved in cell–cell communication (28) in general and those cross-reacting with acyl-HSL receptor receptors in particular. Our analysis revealed that HDF is unstable and oxidizes to isatin, whereby the latter does not induce LuxR-mediated activity suggesting that HDF acts in a specific manner.

We found higher concentrations of HDF in cell extracts relative to acyl-HSL and 3-OH PAME in wild-type cells of *R. solanacearum* by a factor of 100 and even higher upon full induction of *hrpB* and addition of tryptophan that we have shown to represent the precursor molecule of HDF. The increased production of HDF in the presence tryptophan might thereby be of relevance during plant infection, where the amino acid might become available to the pathogen from the host (29). The production of a probably relatively high local concentration of HDF that we expect *in situ* is in line with a role of interfering with quorum-sensing circuits of coexisting bacteria rather than acting on the endogenous ones (22, 23). Because *V. fischeri*, the LuxR receptor of which is so far the only protein that we found inducible by HDF is not expected to coexist in the same habitat as *R. solanacearum*, it will be interesting to test other plant-associated bacteria that might profit from the pathogen's plant attack during infection for *luxR*-mediated HDF effects and phenotypes during plant infections. In this context it is interesting to note, that we found a decrease of reporter gene activity of a LuxR homolog of *Agrobacterium* (21) which might indicate that HDF has a modulating activity on exogenous LuxR homologs besides its induction potential. Further investigations are necessary to test other plant associated bacteria that were occasionally observed to occur in *R. solanacearum* infected tissues (N. Peeters, personal communication) for interference with their quorum-sensing system and multiplication upon infection. The identification of HDF will greatly facilitate future studies to unravel the contribution of HDF-dependent signaling to bacterial infection.

Experimental Procedures

Bacterial Strains and Growth Conditions. Wild-type strain *R. solanacearum* GMI1000 and the GMI1525 derivative containing a mutation in *hrpB* are the strains described (12, 30). GMI1728 carries plasmid pAM5, which harbors a cloned copy of *hrpB* (13). GRS407 was obtained as described (12) and resulted in a GMI1000 mutant disrupted in its RSp0694 gene. *R. solanacearum* was grown on complete medium B for plate growth and on minimal medium supplemented with 20 mM glutamate at 30°C under aerobic conditions for liquid cultures (30). *E. coli* cells were grown on Luria-Bertani (LB) medium at 37°C. For expression studies, *E. coli* containing the pcdna2.1 plasmid (Invitrogen) carrying a DNA insert starting 1.4 kb upstream of the RSp0693 start codon and ending 1.1 kb downstream of the RSp0698 stop codon were used. This strain was grown on M9 minimal medium. For identity and references of the biosensors used see below. Antibiotics were used at the following concentrations: 100 μg/ml ampicillin, 10 μg/ml tetracycline, 10 μg/ml gentamycin, and 40 μg/ml spectinomycin.

Extraction, UV Detection, and Purification of HDF. *R. solanacearum* cultures were grown in minimal medium and centrifuged at 4,000 × *g* for 10 min. Culture supernatants were passed through a 0.2-μm-pore-size filter and extracted twice with equal volumes of ethyl acetate plus glacial acetic acid at 0.1 ml/liter. Remaining water from the organic phase was removed with magnesium sulfate, and ethyl acetate was removed by rotary evaporation at 40–45°C. Finally, samples were dissolved in acetonitrile to obtain a 1,000× concentrated solution. Fractions were applied to TLC on aluminium sheets, 20 × 20 cm, RP-18 F_{254} (Merck, Darmstadt, Germany) and chromatograms were developed by using 60% methanol as solvent. Spots were visualized by UV irradiation (365 nm). For HLPC analysis, the concentrated extracts of culture supernatants from different *R. solanacearum* strains were applied to a C8 reverse-phase analytic HPLC column (Uptisphere C8, 125 × 4.6 mm reverse-phase column; Interchim, France) and eluted with a linear gradient of acetonitrile in water (5–100%) at a flow rate of 1 $ml \cdot min^{-1}$ over a 12-min period monitored at 191 and 210 nm. The eluant was collected as 0.2 ml fractions, and positive fractions were identified by using TLC RP-18, as described above.

For purification of HDF, overnight cultures of *R. solanacearum* GMI1728 were supplemented with 5 mM tryptophan when cell density reached an optical density OD_{600} of 0.8 and were cultured for 6 h before supernatant was extracted. During the first step of HDF purification, preparative TLC was used applying the conditions mentioned above. The spot of interest (Rf = 0.7) was scraped and separated from the silica gel by three successive extractions using 500 μl of acetonitrile. After concentration by evaporation, the fraction was applied to TLC on Kieselgel 60 F_{254} (20 × 20 cm, Merck), and the chromatogram was developed by using dichloromethane–glacial acetic acid (99:1). The spot (Rf = 0.4) was visualized and scraped as described above.

NMR Spectroscopy. NMR experiments of HDF were carried out at 18°C on a Bruker AVANCE spectrometer operating at 600.13 MHz (proton frequency) with a 5-mm triple resonance TCi ^{1}H ^{13}C ^{15}N, pulsed field *z*-gradient cryoprobe. HDF was dissolved in degassed acetonitrile-d_3 and conditioned under argon into the NMR tube. Chemical shifts were expressed in ppm with respect to TMS, by using acetonitrile signals as an internal reference (δ_H/TMS 1.94 ppm and δ_{13C}/TMS 118.69 ppm). One dimensional ^{1}H spectra were collected by using a sweep width of 7183 Hz, 32768 complex points and a repetition delay of 2 s between each scan. 1D ^{13}C spectra were collected by using a sweep width of 36,231 Hz, 98,304 complex points, and proton decoupling during acquisition was performed by using WALTZ-16 scheme at the proton frequency. Two dimensional ^{1}H-detected spectra, ^{1}H-^{1}H DQF-COSY (31), HMBC (32), HSQC (33), H2BC (14), ^{1}H-^{15}N and ^{1}H-^{13}C HN(CO)CA (34), were acquired by using 2048 complex points, with a spectral width of 9615 Hz and a relaxation delay of 2 s. ^{1}H-^{1}H DQF-COSY was performed by using 256 complex data points in *t1* and 32 scans per increment, whereas HSQC, HMBC, and H2BC were acquired with a sweep width of 33557 Hz in the carbon dimension, 128 complex data points in *t1* and 16, 128, and 128 scans per increment, respectively. HMBC spectrum was carbon decoupled during acquisition with GARP scheme and a refocusing delay of 0.061 s before acquisition. 2D ^{1}H-^{13}C and ^{1}H-^{15}N HN(CO)CA were performed with 256

transients per increment and 40 complex data points in *t1* (sweep width of 2189 Hz) and 64 complex data points in *t1* (sweep width of 4831 Hz), respectively. All spectra were zero-filled with 4,096 × 2,048 data points (F2 × F1) and apodized by using a shifted squared sinebell window function in each dimension. Data were processed by using Bruker TOPSPIN software.

Chemical Synthesis of HDF. Synthesis of 3-hydroxy-indolin-2-one was realized according to Usami *et al*. (16). ^{1}H NMR (CD_3OD, 300 MHz): 7.26 (1H, d, *J* 7.5), 7.14 (1H, dd, *J* 7.5, 7.5), 6.93 (1H, ddd, *J* 7.5, 7.5, 0.9), 6.76 (1H, d, *J* 7.5), 4.82 (1H, s_{br}).

CD Spectroscopy. CD experiments were carried out at room temperature on a Jobin-Yvon Mark VI spectropolarimeter, with wavelengths in the range of 220–340 nm. Spectra were acquired by using an integration time of 1 s and a scanning speed of 0.2 nm/s, by accumulation of three scans. HDF was dissolved in ethanol and analyzed in a 0.1 cm cell. The spectrum was baseline-corrected with the spectrum of ethanol recorded in the same conditions.

Mass Spectrometry. High resolution LC-MS was used to determine the chemical composition of purified HDF. LC-MS was also used to quantify HDF in cell extracts in addition to 3-OH-PAME, and *N*-acyl-HSL. Analyses were carried out with a Rheos 2200 HPLC system (Flux Instruments, Basel, Switzerland) coupled to an LTQ-Orbitrap (Thermo Fisher Scientific, Waltham, MA), which was equipped with an atmospheric pressure chemical ionization probe. The compounds were separated with a Gemini C18 analytical column (150 × 2.0 mm, particle size 3 mm; Phenomenex, Torrance, CA, USA) at a flow rate of 200 ml·min^{-1}. Injection volume was 10 μl. MS analysis was done in the positive FTMS mode at a resolution of 60,000. The analytes were identified by the exact masses of the corresponding $[M+H]^+$ ions. For each compound class, individual LC-MS methods were applied (see SI Table 2).

Biosensor Assay. The following *luxR*-biosensor strains were used in this study: *E. coli* pSB401 and pSB403 containing *luxR* from *V. fischeri* (19), *E. coli* MT102 (pJBA-132) (20) *Pseudomonas syringae* BHSL (pBQ9) (35), *Pseudomonas putida* F117 (pKR-C12) (36), *P. putida* F117 (pAS-C8) (36), *Agrobacterium tumefaciens* NTL4 (pCF218)(pCF372) (21), *E. coli* DH5a (pSCR1) containing *luxR* from *Burkholderia cepacia* (37), as well as *Chromobacterium violaceum* CV026 (38) and grown as described. To analyze LuxR-based reporter activities, purified HDF from *R. solanacearum* (1–3 μl, 700 μM) was spotted on individual small Petri dishes filled with a first layer of LB medium. Plates were then covered with a second layer of LB soft agar containing an aliquot of the corresponding biosensor strain in exponential growth phase. Plates were incubated overnight at 30°C in the dark before pigment, GFP, bioluminescence production or β-galactosidase activity were observed, respectively. Synthetic acyl-HSL were used as positive controls and were purchased from Fluka.

Quantitative assays with *E. coli* DH5a pSB401 were performed essentially as described before (19). Briefly, samples were spotted on 96-well microtiter plates, and covered with 200 μl of an *E. coli* DH5α (pSB401) overnight culture, previously diluted to an optical density at 600 nm of ≈0.1. Plates were incubated in the dark at 30°C for 18 h, and bioluminescence was measured in a microtiter plate reader (Victor 3, Perkin–Elmer, Waltham, MA). Calibration curves were obtained with synthetic *N*-hexanoyl-HSL and *N*-3-oxo-hexanoyl-HSL and resulted in dose dependent light induction as described (19). For other LuxR-homolog activities, assay tubes were used instead of microtiter plates and quantifications were performed as described before (21). Inhibitory activities were assayed essentially in the same way, by mixing known quantities of the corresponding acyl-HSL and known quantities of HDF.

We thank the Centre National de la Recherche Scientifique (CNRS), the Max-Planck-Gesellschaft (MPG), and ETH Zurich for financial support. The NMR equipment was funded by means of European structural funds, CNRS, and the Région Midi-Pyrénées funds as part of the 2000–2006 CPER program.

1. Hayward AC (2000) in *Encyclopedia of Microbiology* (Academic, San Diego), pp. 32–42.
2. Genin S, Boucher C (2004) *Annu Rev Phytopathol* 42:107–134.
3. Schell MA (2000) *Annu Rev Phytopath* 38:263–292.
4. Aldon D, Brito B, Boucher C, Genin S (2000) *EMBO J* 19:2304–2314.
5. Brito B, Aldon D, Barberis P, Boucher C, Genin S (2002) *Mol Plant Microbe Interact* 15:109–119.
6. Cunnac S, Boucher C, Genin S (2004) *J Bacteriol* 186:2309–2318.
7. Occhialini A, Cunnac S, Reymond N, Genin S, Boucher C (2005) *Mol Plant Microbe Interact* 18:938–949.
8. Salanoubat M, Genin S, Artiguenave F, Gouzy J, Mangenot S, Arlat M, Billault A, Brottier P, Camus JC, Cattolico L , *et al*. (2002) *Nature* 415:497–502.
9. Cunnac S, Occhialini A, Barberis P, Boucher C, Genin S (2004) *Mol Microbiol* 53:115–128.
10. Fuqua C, Greenberg EP (2002) *Nat Rev Mol Cell Biol* 3:685–695.
11. Forouhar F, Anderson JL, Mowat CG, Vorobiev SM, Hussain A, Abashidze M, Bruckmann C, Thackray SJ, Seetharaman J, Tucker T, *et al*. (2007) *Proc Natl Acad Sci USA* 104:473–478.
12. Genin S, Gough CL, Zischek C, Boucher CA (1992) *Mol Microbiol* 6:3065–3076.
13. Gueneron M, Timmers AC, Boucher C, Arlat M (2000) *Mol Microbiol* 36:261–277.
14. Nyberg NT, Duus JO, Sorensen OW (2005) *J Am Chem Soc* 127:6154–6155.
15. Sonderegger OJ, Bürgi T, Limbach LK, Baiker A (2004) *J Mol Cat A* 217:93–101.
16. Usami N, Kitahara K, Ishikura S, Nagano M, Sakai S, Hara A (2001) *Eur J Biochem* 268:5755–5763.
17. Degrassi G, Aguilar C, Bosco M, Zahariev S, Pongor S, Venturi V (2002) *Curr Microbiol* 45:250–254.
18. Holden MT, Ram Chhabra, S., de Nys R, Stead P, Bainton NJ, Hill PJ, Manefield M, Kumar N, Labatte M, England D, *et al*. (1999) *Mol Microbiol* 33:1254–1266.
19. Winson MK, Swift S, Fish L, Throup JP, Jorgensen F, Chhabra SR, Bycroft BW, Williams P, Stewart GS (1998) *FEMS Microbiol Lett* 163:185–192.
20. Andersen JB, Heydorn A, Hentzer M, Eberl L, Geisenberger O, Christensen BB, Molin S, Givskov M (2001) *Appl Environ Microbiol* 67:575–585.
21. Zhu J, Beaber JW, More MI, Fuqua C, Eberhard A, Winans SC (1998) *J Bacteriol* 180:5398–5405.
22. Flavier AB, Ganova-Raeva LM, Schell MA, Denny TP (1997) *J Bacteriol* 179:7089–7097.
23. Flavier AB, Clough SJ, Schell MA, Denny TP (1997) *Mol Microbiol* 26:251–259.
24. Mukaihara T, Tamura N, Murata Y, Iwabuchi M (2004) *Mol Microbiol* 54:863–875.
25. Guidot A, Prior P, Schoenfeld J, Carrere S, Genin S, Boucher C (2007) *J Bacteriol* 189:377–387.
26. Da Silva AC, Ferro JA, Reinach FC, Farah CS, Furlan LR, Quaggio RB, Monteiro-Vitorello CB, Van Sluys MA, Almeida NF, Alves, L. M. *et al*. (2002) *Nature* 417:459–463.
27. Müh U, Hare BJ, Duerkop BA, Schuster M, Hanzelka BL, Heim R, Olson ER, Greenberg EP (2006) *Proc Natl Acad Sci USA* 103:16948–16952.
28. Waters CM, Bassler BL (2005) *Annu Rev Cell Dev Biol* 21:319–346.
29. Jaeger CH, Lindow SE, Miller S, Clark E, Firestone MK (1999) *Appl Environ Microbiol* 65:2685–2690.
30. Boucher CA, Barberis PA, Trigalet AP, Démery DA (1985) *J Gen Microbiol* 131:2449–2457.
31. Ancian B, Bourgeois I, Dauphin, J-F, Shaw AA (1997) *J Magn Res* 125:348–354.
32. Bax A, Griffey RH, Hawkins BL (1983) *J Magn Res* 55:301–315.
33. Schleucher J, Schwendinger M, Sattler M, Schmidt P, Schedletzky O, Glaser SJ, Sorensen OW, Griesinger C (1994) *J Biomol NMR* 4:301–306.
34. Kay LE, Xu GY, Yamazaki T (1994) *J Magn Res* 109:129–133.
35. Karamanoli K, Lindow SE (2006) *Appl Environ Microbiol* 72:7678–7686.
36. Steidle A, Sigl K, Schuhegger R, Ihring A, Schmid M, Gantner S, Stoffels M, Riedel K, Givskov M, Hartmann A, *et al*. (2001) *Appl Environ Microbiol* 67:5761–5770.
37. Aguilar C, Bertani I, Venturi V (2003) *Appl Environ Microbiol* 69:1739–1747.
38. McClean KH, Winson MK, Fish L, Taylor A, Chhabra SR, Camara M, Daykin M, Lamb JH, Swift S, Bycroft BW, *et al*. (1997) *Microbiol* 143:3703–3711.